Journal of Catalysis 358 (2018) 27–34

Contents lists available at ScienceDirect

Journal of Catalysis

journal homepage: www.elsevier.com/locate/jcat

In situ monitoring of the phenomenon of electrochemical promotion of catalysis

J.P. Espinós [a], V.J. Rico [a], J. González-Cobos [b], J.R. Sánchez-Valencia [a], V. Pérez-Dieste [c], C. Escudero [c], A. de Lucas-Consuegra [d,*], A.R. González-Elipe [a,*]

[a] Institute of Materials Science of Sevilla, University of Sevilla-CSIC, Avenida Americo Vespuccio 49, 41092 Sevilla, Spain
[b] Institute of Chemical Research of Catalonia (ICIQ), Ave. Paisos Catalans 16, 43007 Tarragona, Spain
[c] ALBA Synchrotron Light Source, Carres de la Llum, 2-26, 08290 Cerdanyola del Vallés, Barcelona, Spain
[d] Department of Chemical Engineering, School of Chemical Sciences, University of Castilla-La Mancha, Ave. Camilo José Cela 12, 13005 Ciudad Real, Spain

ARTICLE INFO

Article history:
Received 13 June 2017
Revised 25 September 2017
Accepted 26 November 2017
Available online 9 December 2017

Keywords:
Electrochemical promotion
Spillover
Alkaline conductors
XPS
NAPP
Synchrotron analysis
Ni catalyst
Glancing angle deposition

ABSTRACT

In this work we investigate by in-situ near-ambient pressure photoemission (NAPP) spectroscopy the phenomenon of Electrochemical Promotion of Catalysis (EPOC). We studied the reduction and diffusion kinetics of alkaline ions in a solid electrolyte cell formed by a nickel electrode supported on K^+-β-alumina electrolyte. Experiments in ultra-high vacuum and in the presence of steam showed that the amount of potassium atoms supplied to the surface is probably affected by nickel electronic modifications induced by adsorbed OH^- groups. It was also deduced that part of the segregated potassium would be adsorbed at inner interfaces where it would be inaccessible to the photoelectron analyzer. A migration mechanism of the promoter is proposed consisting in: (i) the electrochemical reduction of the alkali ions (potassium) at the Ni/solid electrolyte/gas interface; (ii) the spillover of potassium atoms onto the Ni gas-exposed surface; and (iii) the diffusion of potassium atoms to Ni inner grain boundary interfaces.

1. Introduction

The Electrochemical Promotion of Catalysis (EPOC) concept has opened a new way of improving activity and selectivity of a heterogeneous catalytic reaction [1–3]. EPOC is based on the electrochemical activation of a catalyst film in contact with a solid electrolyte material (e.g., H^+, Na^+, K^+, O^{2-} ionic conductors) that acts as a source of promoter ions. This phenomenon is not limited to a particular kind of catalyst, solid electrolyte material or chemical reaction and has been proved in a wide variety of systems [1]. To unravel its operating mechanisms, several experimental procedures have been utilized including adsorption-desorption techniques, work function measurements, isotope labeling, cyclic voltammetry, electronic microscopy, impedance spectroscopy and other spectroscopic techniques [1,4]. Of particular relevance for the present investigation are previous works using X-ray photoelectron (XPS) and Auger electron spectroscopies (AES) carried out by the group of Lambert et al., who analyzed EPOC systems based on alkaline (Na^+ and K^+) ionic conductors and Pt [5–7], Rh [8,9] or Cu [10,11] catalyst films. In these studies, the solid electrolyte cells were initially exposed to EPOC reaction conditions in the pre-chamber of an electron spectrometer and then transferred to the ultra-high vacuum analysis chamber to collect the XP spectra. Although these works were not carried out under real "in operando" conditions, they showed that upon cathodic polarization the alkaline ions (M^+) of the solid electrolyte migrate to the three-phase boundary (tpb), i.e., metal electrode/solid electrolyte/gas interface, where they become reduced to their elemental state (M) (i.e., reaction (1)), and then spill-over to the gas-exposed metal surface where they become adsorbed in neutral form.

$$M^+ + e^- \rightarrow M_{ads} \quad (1)$$

The present work using Near Ambient Pressure Photoemission Electron Spectroscopy (NAPP) goes a step forward vs. these previous studies through the application of an experimental approach enabling the following:

(i) To perform photoemission measurements under polarization in the same reactor chamber and conditions closer to those of an "operando" methodology [12].

* Corresponding authors.
E-mail addresses: Antonio.Lconsuegra@uclm.es (A. de Lucas-Consuegra), arge@icmse.csic.es (A.R. González-Elipe).

https://doi.org/10.1016/j.jcat.2017.11.027
0021-9517/

(ii) To work at near ambient pressure, i.e. under reaction conditions similar to those encountered in EPOC electrochemical cell reactors.

The present study has been carried out in the context of previous EPOC works carried out by our group on catalytic hydrocarbon and alcohol reforming reactions [13–15]. Herein, by working under in-situ NAPP conditions we have gained a better understanding of the alkaline ion/metal diffusion processes by monitoring the potassium supply/removal under cathodic/anodic polarizations, i.e., in the course of the electric polarizations. Namely, we have found new evidences about potassium segregation onto the catalyst surface and back to the electrolyte when applying a negative/positive potential to the alkaline solid electrochemical cell. In particular, we have comparatively analyzed the kinetics of potassium surface segregation followed by NAPP as a function of atmosphere with the time evolution of the cell electrical signals (i.e., intensity and voltage) simultaneously measured with a potentiostat-galvanostat. The differences found between these two time-dependent signals have been rationalized with a three-step potassium reaction and migration mechanism during polarization. We propose that this systematic comparison can be a powerful methodology not only to understand the EPOC phenomenon, but also for other experiments in fields such as fuel cells, photovoltaic cells, batteries, corrosion and, in general, electrochemical systems where diffusion processes are key issues for device performance.

2. Experimental

2.1. Preparation of the electrochemical catalyst

The solid electrolyte cell was formed by a Ni film deposited on a side of a 19-mm-diameter, 1-mm-thick K-βAl_2O_3 (Ionotec) disc (7.9 mm diameter, geometric area = 2.01 cm^2) acting as electrolyte. The catalytically inert Au counter/reference (C/R) electrode was deposited on the other side of the electrolyte by applying a thin gold paste coat, followed by calcination at high temperature. Then, the active Ni catalyst film, which also behaves as a working electrode (W), was deposited on the other side of the electrolyte by a modification of the classical physical vapor deposition (PVD) technique, called oblique or glancing angle deposition (OAD or GLAD) [16,17]. By this method, the substrate (K-βAl_2O_3) is placed in an oblique angle configuration with respect to the evaporated flux of deposited material (Ni) to enhance nanostructuration effects induced by the shadowing effects occurring during film growth [18]. As a result, a highly porous film, characterized by a high surface area and a controlled microstructure formed by tilted nanocolumns, was obtained. This kind of catalyst morphology can be of special interest in electrochemically assisted catalytic processes for H_2 production and storage [14]. In the present study, the Ni catalyst film was deposited at a zenithal evaporation angle $\alpha = 80°$. As determined by Rutherford back scattering spectroscopy (RBS), these films presented an equivalent mass thickness of 900 nm (i.e., equivalent thickness if the film were compact). A SEM micrograph of the nanostructured Ni film is reported in Fig. 1a. This figure clearly shows that most nickel agglomerates in the form of nanocolumnar patches, while a continuous Ni layer also covers the substrate (see results). Additional characterization and electrocatalytic behavior of these electrode thin films can be found in previous works [14,16].

2.2. Near-ambient pressure photoemission spectroscopy measurements

For the NAPP experiments, the Ni/K-βAl_2O_3/Au electrocatalytic cell was incorporated in a special sample holder (see scheme in Fig. 1b). The sample, a circular pellet of K-βAl_2O_3 with its top side coated with the porous Ni film and a gold dense film on the bottom, was silver glued to the sample holder through its back face. The sample holder consisted of a cylindrical stainless steel piece fully surrounding the back and lateral sides of the sample. It was connected with a thin silver thread (0.2 mm) to the active terminal of a potentiostat/galvanostat (Vertex model, Ivium Technologies). On the top side, a small drop of silver paste (4 mm^2 contact area) was deposited on the outer edge of the circular Ni electrode and then electrically contacted through a small spiral silver thread that was immersed in the silver paste till its drying and curing at room temperature. This second thread was connected to the second terminal of the potenciostat and grounded. This configuration means that, whatever the bias voltage applied to the Au counter electrode, the Ni electrode was always earthed, as required for referencing the binding energy scale of the photoelectron energy analyzer. A picture of this sample holder configuration is shown in Fig. 1c.

The NAPP spectrometer was located at the BL-24 CIRCE undulator beamline, in the ALBA synchrotron light source (Sant Cugat del Vallés, Spain); it is equipped with a Phoibos NAP150 XPS analyzer (SPECS) and a differential pumping system for operating at a given pressure in the analysis chamber. The beam spot size at the sample position was around $100 \times 20\ \mu m^2$. Samples were excited with photons of two different energies: 460 eV and 1170 eV. The emitted photoelectrons were analyzed with a pass energy of 10 eV. K/Ni atomic ratios were determined from the K2p and Ni3p spectra measured with hν = 460 eV, while C/Ni ratios were determined from the C1s and Ni2p spectra measured with hν = 1170 eV. For a semiquantitative evaluation of spectra, raw areas under the peaks were corrected for the photoionization cross sections of each electronic level [19] and the escape depth of photoelectrons [20].

Generally, spectra were recorded at the final state conditions of the experiments. In addition, the maximum of the K2p peak signal was continuously recorded as a function of time together with the current (I) and/or potential (V) applied and/or monitored with the potentiostat-galvanosotat. All the experiments were carried out at the optimal temperature of 280 °C, as determined in previous studies [14], and two reaction atmospheres: under the presence of water vapor as an active adsorbate, denoted as "water conditions", (water pressure of 10^{-2} mbar), and under absence of any active adsorbate, denoted as "high vacuum" (residual pressure in the chamber of 10^{-7} mbar).

3. Results and discussion

A common feature of reforming reactions (for hydrocarbons or alcohols) is the use of water vapor as a second reactant. Water is also of paramount importance for the removal of deposited carbonaceous species on catalytic active sites [15,21]. Therefore, a first experiment was dedicated to condition the electrocatalyst surface and to monitor the evolution of the carbon residues on the Ni catalyst surface exposed to water vapor at 280 °C in the absence of any applied voltage, i.e., under open circuit conditions. Carbon residues were inevitably incorporated to the Ni catalyst surface during film preparation and afterwards during the manipulation of the cell in air. The collected NAPP spectra reported in Fig. 2 were obtained along 50 min and show that the intensity of the C1s signal of the adsorbed adventitious carbon progressively decreased up to reaching an almost negligible intensity in the steady state. This pre-treatment allowed obtaining an almost clean Ni catalyst film. The Ni2p signal of metallic nickel, characterized by a BE of 852.7 eV [22] did not undergo any significant modification in shape, although its intensity slightly increased as a result of this water vapor conditioning treatment. Meanwhile, a small O1s signal due to OH^- or similar functional groups was also recorded after that

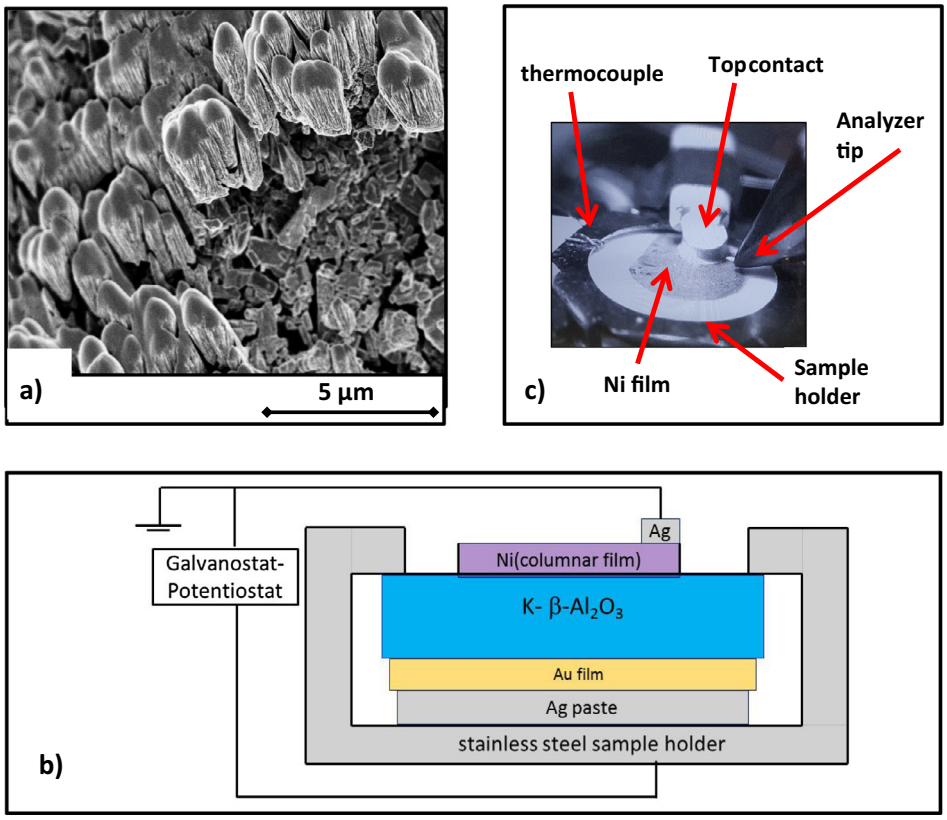

Fig. 1. (a) SEM micrograph of the nanostructured Ni electrode prepared by OAD on the ion conductor support. (b) Scheme of sample holder with the electrochemical cell attached to it. (c) Actual photograph of the device with indication of the constituent parts.

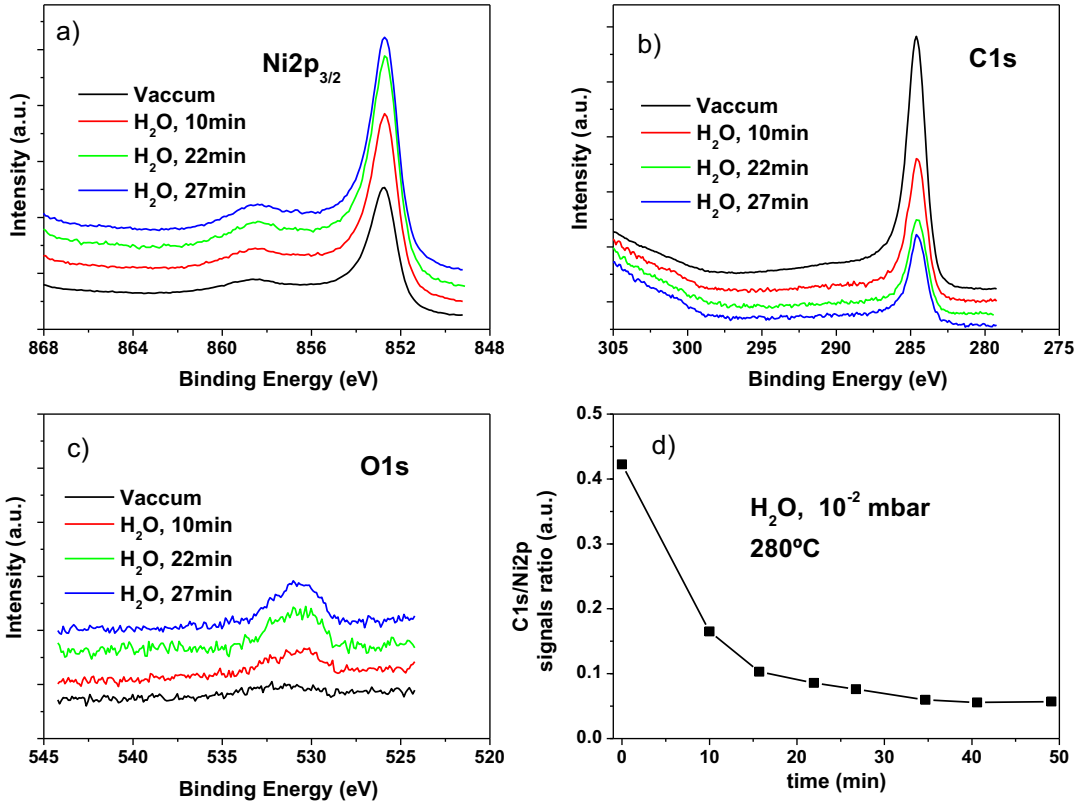

Fig. 2. Evolution of NAPP signals recorded for the electrocatalyst exposed to water vapor at 280 °C for increasing periods. Spectra are reported for the Ni2p (a), C1s (b) and O1s (c) peaks measured with photons of 1170 eV. The evolution of the C1s/Ni2p area ratio is included in (d).

treatment. These preliminary results revealed an efficient carbon removal by reaction with water vapor, a well-established catalytic reaction on Ni [23,24]. From this preliminary analysis it is also of relevance that no signals corresponding to Al^{3+}/O^{2-} ions or Ag atoms could be detected, indicating that the nanostructured nickel catalyst-electrode covered efficiently the solid electrolyte support and that silver atoms from the paste (see Fig. 1b) did not migrate to the NAPP analysis area.

Fig. 3 shows the spectra recorded for this pre-conditioned sample after applying a positive (+2 V) and then a negative voltage of (−2 V), either in vacuum (i.e., 10^{-7} mbar) or in the presence of 10^{-2} mbar water vapor. This polarization protocol is typical of EPOC studies with alkaline ionic conductors, where the solid electrolyte cell is first positively polarized to create a clean catalyst surface free from alkali promoters and then negatively to electrochemically supply alkali species. The constant shape of the Ni2p signals observed for all the recorded spectra indicated that the catalyst exposed surface remained unaltered after the treatments and that it consisted of metallic nickel (BEs of 852.7 and 66.2 eV and FWHM of 1.42 and 3.55 eV for the $Ni2p_{3/2}$ and Ni3p peaks, respectively [22]). Meanwhile, a very intense K2p signal (see Fig. 3b) suddenly developed when applying −2 V and disappeared almost immediately when switching the voltage to +2 V. This behavior was completely reversible, although the intensity of the K2p signal was higher when the experiment was carried out in the presence of water vapor vs. vacuum (K/Ni atomic ratios, determined from the K2p and Ni3p spectra measured with hv = 460 eV, were 0.4 vs. 0.16, respectively). This can be attributed to an enhanced stabilization of potassium onto the Ni catalyst surface due to the adsorbed OH^- groups coming from water. A small decrease in the C1s and Ni2p/Ni3p signals occurred with both atmospheres under application of −2 V, a feature that we attribute to photoelectrons screening by the segregated potassium. On the other hand, an increase in the O1s signal (Fig. 3c) was observed upon negative polarization under water atmosphere. This behavior is in good agreement with the EPOC theory and can be attributed to modifications in the catalyst chemisorption capability in the presence of the electrochemical promoter [25]. In our experiment, water chemisorption (electron acceptor) would be enhanced during negative polarization, i.e., in the presence of potassium, in agreement with previous studies about alkali promotion of conventional catalysts and EPOC systems [13,26,27]. It should be noted that the K2p signal had BEs in the range 294.1–294.6 eV, depending on the composition of the gas phase and thus the concentration of K. These values are characteristic of elemental potassium adsorbed on metal surfaces [28,29].

In previous works with similar alkaline solid electrolyte cells [6–8,10], the application of a negative voltage to the catalyst film led to the appearance of two alkaline XPS signals. The first one, corresponding to the alkali elemental form (K^0 or Na^0), presented a constant BE and an increasing intensity when the applied potential decreased. It was attributed to alkali atoms adsorbed on the catalyst surface. The second one, at higher binding energies, corresponded to the ionic form (K^+ or Na^+), had a constant intensity and was attributed to ionic species localized at the solid electrolyte/catalyst/gas phase interface. Their detection was possible due to cracks and pores in the metal catalyst film which would not completely cover the electrolyte. In the present study, the absence of this second alkaline signal, as well as any other signal coming from the Al_2O_3 support (e.g., Al^{3+} ions) confirmed that the solid electrolyte was fully covered by the nickel catalyst film.

The observed segregation of potassium in this experiment was practically instantaneous when the voltage was switched from 2 V to −2 V and the evolution of the K2p signal could not be monitored as a function of time. However, the rapid time evolution of the electric current could be monitored with the potentiostat for

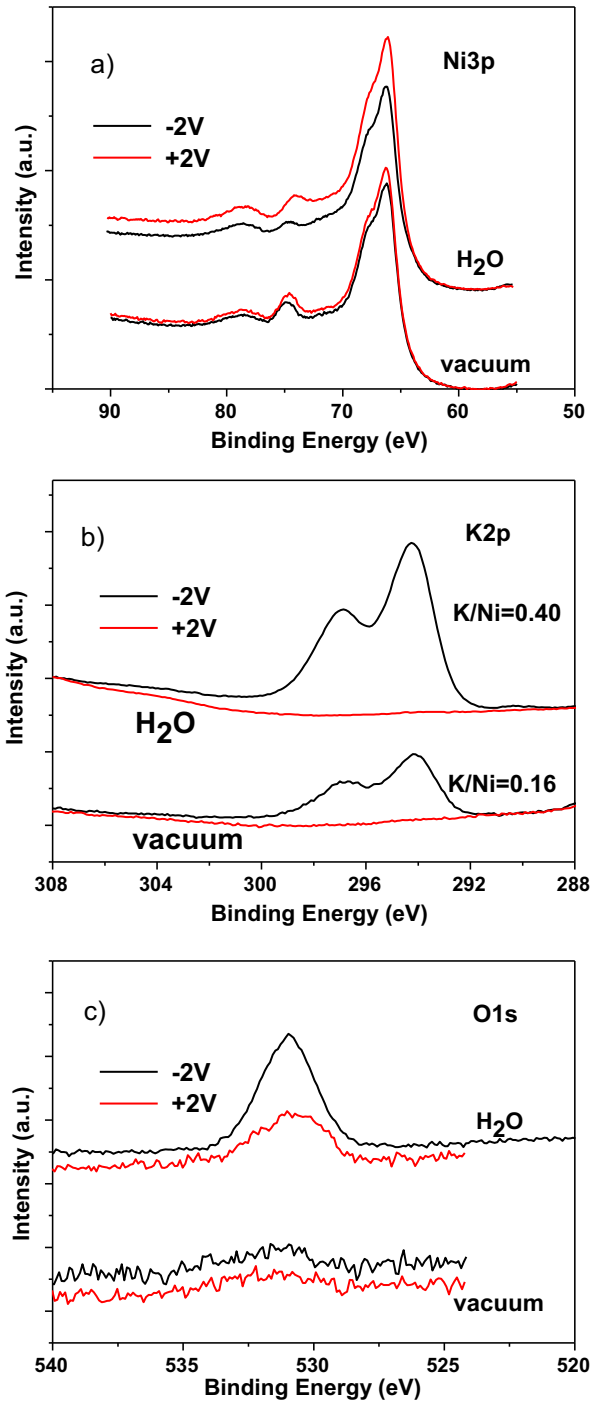

Fig. 3. (a) Ni3p spectra recorded "in situ" at 280 °C for the electrocatalyst exposed to water vapor and vacuum conditions after applying +2 V and −2 V, as indicated. (b) Evolution of the K2p signals during the same experiments. (c) Idem for the O1s spectra. Ni3p and K2p spectra were recorded with hv = 460 eV, while O1s was recorded with hv = 1170 eV.

the two applied potentials (see supporting information, Fig. S1). In this case I(t) followed a sharp exponential decay that reached zero after (0.5–1) min. These curves reflect the alkali ions reduction (negative currents) and metallic potassium oxidation (positive currents) rates at the tbp, obtained at each polarization (negative or positive) according to Faraday law:

$$\text{Potassium oxidation/reduction rate/mol}_{K+}\ s^{-1} = \frac{I}{nF} \qquad (2)$$

where I is the varying current value, n is the potassium ion charge (+1) and F is the Faraday constant (96,485 C $mol_{e^-}^{-1}$).

Fig. 4 shows the evolution of both K2p and electric current intensity signals simultaneously recorded as a function of applied voltage from +2 to −2 V (scan rate of 5 mV s^{-1}) during cyclic voltammetry experiments carried out in high vacuum and in the presence of water vapor. The two kinds of curves obtained under these conditions presented a cyclic behavior and a clear hysteresis. In all cases there was total absence of potassium on the catalyst surface upon the initial polarization at +2 V. During the negative polarization scan (from +2 to −2 V), the negative current values observed in Fig. 4b suggests that potassium ions were reduced to metallic potassium, very likely at the tpb (reaction 1). This metallic potassium seems to migrate from the tpb to the nickel gas exposed surface as observed by the increase in the K2p signal in Fig. 4a. During the cathodic scan, a voltammetry peak at around −1.2 V coincides with a decrease in the slope of the K2p signal evolution. At this potential, K2p intensity almost reached its maximum value, even though rather high negative currents continued to be recorded up to −2 V. We advance that these different evolutions might be due to the existence of an additional diffusion mechanism of metallic potassium that would migrate from the Ni catalyst surface to inter-grain boundaries and interfaces in the bulk of the film where it would not be detectable by photoemission. On the other hand, during the anodic scan from −2 V to −1 V, low intensity (but still negative) currents were continuously obtained. We presume that potassium ions are still reduced at the tpb (reaction 1)

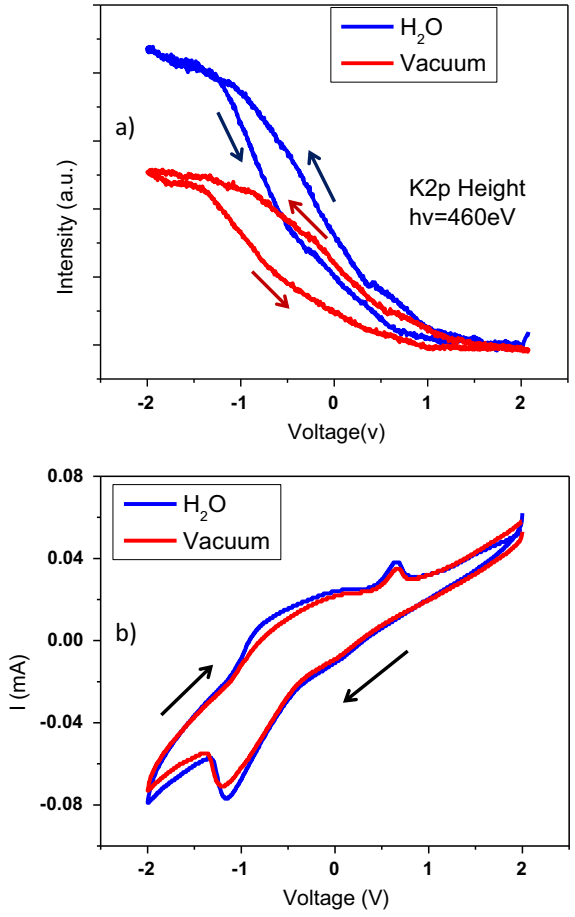

Fig. 4. (a) I-V voltammogram curves recorded with the potentiostat for the electrocatalyst in vacuum or exposed to 10^{-2} mbar water vapor. (b) Evolution of the K2p signal intensity "in-situ" measured by NAPP while changing the voltage in the same experiments.

and that this second diffusion process further depletes the amount of potassium directly exposed at the Ni surface. At potentials higher than −1 V, positive current values were obtained during the anodic scan (from −1 V to +2 V), indicating that the opposite processes were taking place, i.e., metallic potassium atoms migrated from the Ni film to the tpb from where, after oxidation to cationic form, would return back to the solid electrolyte. In this potential range (−1 V to +2 V) the K2p signal decreased with a higher rate than in the previous voltage range (−2 V to −1 V), denoting a faster removal of potassium from the surface mediated by a back-reaction (1). As a result, the K2p signal followed a hysteresis curve during the cyclic voltammetry with its lower intensity branch occurring during the back anodic scan (from −2 to 2 V).

During these electrochemically driven processes, the similar shapes of the I-V voltammograms in vacuum and in the presence of water vapor suggest that the involved electrochemical processes were not substantially affected by the presence of water vapor. It is likely that the low partial pressure (10^{-2} mbar) in our experiment limits the concentration of H_2O/OH^- species at the tpb, making that charge-transfer reaction (1) was little affected by the water vapor used in the experiment. This behavior is different than that of previous works in literature [30,31] reporting a clear influence of the gas-phase composition in the current-voltage voltammetry curves under higher gas pressures. It also contrasts with the much higher intensity of the K2p curves recorded in the same experiment in the presence of water (c.f. Fig. 4a), thus suggesting that even if reaction (1) proceeded in a similar way when there was some water in the environment, the adsorption of potassium atoms at the gas-exposed Ni surface was considerably favoured under these conditions. In other words, the partition of metallic potassium between external surface and internal interfaces in the Ni electrodes was extremely sensitive to small amounts of water in the medium. It is noteworthy in this regard that the BE of the K2p signal was higher in vacuum (i.e., up to 294.6 eV) than in the presence of water (294.1 eV), a difference that we relate with an extra adsorption of hydroxyl groups at the nickel surface (c.f., O1s spectrum at 530.9 eV in Fig. 3c) [29]. It is likely that the additional adsorption of polar groups on nickel provides an extra electron density that would induce this change in BE and the observed extra segregation of potassium onto the surface. The interplay between electron density at the catalyst surface, segregation of alkaline atoms and the surface state of adsorbed groups was observed in previous works by XPS. For instance, Lambert et al. [10] showed that under a NO atmosphere and a decreasing catalyst potential (i.e., pumping Na to the catalyst surface) the extra electronic density provided by the alkali atoms strengthens the metal–N bond, contributing to increase NO coverage, and weakens the N—O bond, this facilitating NO dissociation. Analogously, in studies of NO reduction by CO [11] or by C_3H_6 in the presence of O_2 [9], it was shown that the gas phase composition affected not only the Na1s binding energy (depending on the promoter-derived surface compound formed) but also the signal intensity.

Additional evidences about the existence of distinct states of segregated potassium, at the surface or in the bulk of the nickel films, are provided by the experiment depicted in Fig. 5. This experiment was carried out in presence of water and three different polarization steps. Initially, a chronopotentiometry was carried out, by applying to the sample a negative current of −50 μA during c.a. 13 min up to reach a fairly constant voltage close to −2 V (in line with the cyclic voltammetry). Then, the system was kept under open circuit conditions during c.a. 10 min, and finally a positive voltage of +2 V was applied. During the different polarizations steps, the K2p signal and the voltage evolution curves were simultaneously recorded as a function of time. As a reasonable approximation, the current flowing through the system can be taken as a measurement of the potassium ions reduction rate via Eq. (2)

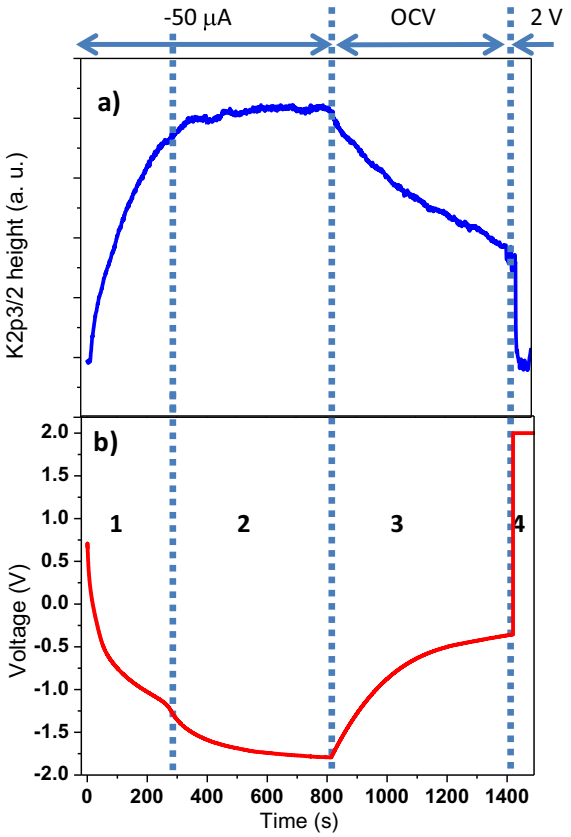

Fig. 5. Time evolutions of the K2p height (a) and voltage (b) on the electrocatalytic system when applying a constant current of −50 μm through the cell (region 1 and 2) and then leaving the system under open circuit conditions to evolve naturally (region 3). The experiment concluded after applying a constant voltage of 2 V to the cell (region 4).

(i.e. 5.2×10^{-10} mol_{K+} s^{-1} for 50 μA), while the kinetic of potassium migration to the gas-exposed surface was determined following the evolution of the K2p signal with time. During the initial galvanostatic application of −50 μA, the K2p signal sharply increased while the potential decreased up to reach a value c.a. −1.2 V (region 1). At this stage, a plateau could be observed in the K2p signal evolution while the potential continued decreasing with a lower slope rate (region 2). It is noteworthy that the change in both signals occurred at c.a. −1.2 V, a potential at which a peak appeared in the cyclic voltammetry curves in Fig. 4b.

To stress these differences we adjusted a time dependent curves in each case with the simplest function providing a good fitting (this does not pretend to be a proper kinetic analysis, for which temperature dependent data should be necessary). The potential and exponential functions shown in Fig. S2 where those that were better adjusted to the K2p intensity and potential curves, respectively. The K2p intensity curve in region 1 could be adjusted with a function of the type t^x ($0.15 < x < 0.20$) (see Supporting information, Fig. S2) while in region 2 the fitting function took the form $t^{0.03}$. Unlike these potential forms for the K2p signal evolution, the voltage curves in Fig. 5b adjusted to a double exponential function with characteristic time constants of 23 s and 195 s (region 1), and 142 s and 195 s (region 2), as shown on Fig. S2 (note that exponential curves describe the voltage evolution during charging/discharging of capacitors). To account for these completely different time evolutions and the previous observations in Fig. 4, we propose that the overall reduction and migration process of ions in EPOC systems comprises the following three consecutive steps:

$$K^+_{electrolyte} + e^- \rightarrow K_{tbp} \quad (3)$$

$$K_{tbp} \rightarrow K_{surf} \quad (4)$$

$$K_{surf} \rightarrow K_{bulk} \quad (5)$$

Eq. (3) accounts for the potassium ions reduction at the tpb, Eq. (4) for the potassium spill over to the gas-exposed surface of the nickel film (traditionally known as backspillover or reverse spillover phenomena on EPOC systems [1]), while Eq. (5) refers the diffusion of potassium to defect sites, grain boundaries dislocations, etc. in the bulk of the nickel thin film electrode. The activation energy of Eq. (5) would be slightly higher than that of Eq. (4) and therefore proceed to a larger extent only after saturation of surface adsorbed states (i.e. K_{surf} in step (3)). In fact, the higher intensity of the K2p signal and its lower BE in the presence of a low partial pressure of water vapor (c.f., Figs. 3 and 4) support the additional stabilization of potassium on the catalyst surface in the presence of adsorbed OH^- groups. It is also noteworthy that equivalent maximum K2p intensities were reached during the cyclic voltammetry (Fig. 4) and the chronopotentiometry (Fig. 5), denoting that the maximum potassium coverage on a given catalyst surface does not depend on the polarization mode (galvanostatic or potentiostatic), but on the reaction conditions, i.e. pressure, temperature, gas composition and final applied electrical potential or current. The mentioned reduction and diffusion processes are schematized in Fig. 6.

Further insights into the diffusion kinetic of potassium can be gained from the analysis of region 3 in Fig. 5 corresponding to open circuit conditions (OCV) when the cell was evolving spontaneously. It should be noted that potassium showed to remain in its metallic state during this OCV step (see Supporting Information, Fig. S3), as well as in the entire study, with BEs in the range 294.1–294.6 eV, while the long stability of K2p signal over time for stable operation conditions disregard its evaporation from its adsorbed state on nickel. It is apparent that potassium disappeared progressively from the Ni catalyst surface and the voltage increased from the final value achieved in region 2 (c.a. −1.8 V) to c.a. −0.5 V in 10 min. In this case, the voltage curve could be adjusted by an exponential function with a characteristic time of 192 s (see supporting information Fig. S2), while the K2p intensity curve could be adjusted with a potential function of the type $t^{-0.50}$ (i.e., that of a classical surface diffusion kinetics [32]). These observations suggest that potassium atoms are removed from the Ni surface becoming incorporated into Ni inner grain boundary interfaces (i.e., beyond the XPS analysis depth) or back migrated to the solid electrolyte. This latter would agree with the observed evolution in cell potential and would imply a slow direct oxidation of potassium with the water vapor always present in the medium. In relation with basic electrocatalysis concepts, the slow potassium diffusion from the catalyst surface would agree with the preservation of a "permanent EPOC" function in many catalytic systems based on alkaline ionic conductors [33,34]. At the end of the experiment in Fig. 5, the final application of 2 V induced the complete electrochemical oxidation and removal of the potassium atoms remaining at the nickel (i.e. back-reactions (3)–(5)), showing an analogous current trend to that in Fig. S1. We propose that the fully reversible behavior of the promoter migration in this process would be responsible for the reversible catalytic rates typically found under EPOC working conditions [13,33,34].

4. Conclusions

The novel experimental approach based on "in situ" photoemission analysis used in the present work has been used for the monitoring of the phenomenon of electrochemical activation of a

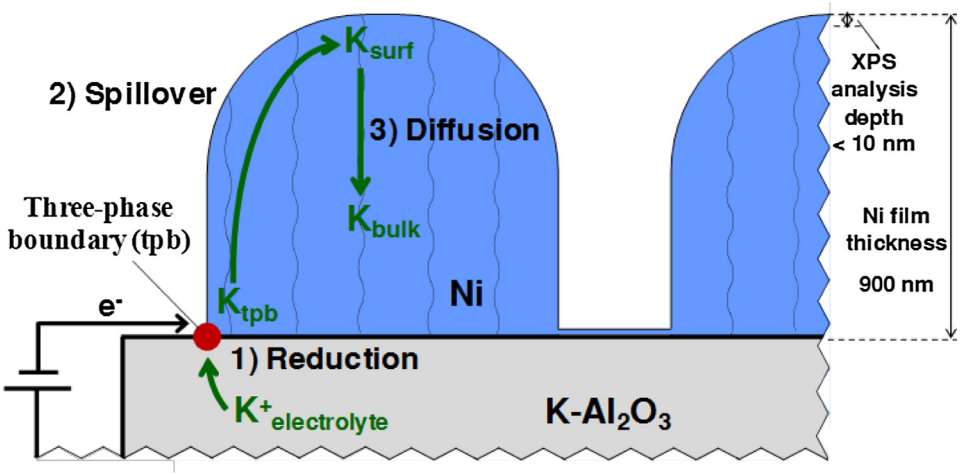

Fig. 6. Schematic representation of the successive potassium reduction/diffusion steps taking place on the solid electrolyte cell upon cathodic polarization: (i) K^+ ions reduction at the Ni/solid electrolyte/gas interface; (ii) spillover of potassium atoms onto the Ni gas-exposed surface; and iii) diffusion of potassium atoms to Ni inner grain boundary interfaces.

catalyst with alkaline ionic conductor materials. In particular, monitoring the kinetics of the reduction and diffusion of alkali ions under EPOC conditions and different polarization modes has provided new evidences about the migration mechanism of the promoters. We have shown that the atomic potassium adsorbed after electrochemical reduction at the tpb may occupy two different sites at the nickel catalyst, a first one at the gas-exposed catalyst surface and the other at the inner catalyst interfaces or grain boundaries. The former is energetically favored, although both states would be in equilibrium and a migration may occur between them in forward and backward directions. Moreover, it is confirmed the mutual adsorption improvement of water/OH- groups and metallic potassium atoms on the catalyst surface. Achieving these conclusions has been possible by the application of a novel methodology involving the simultaneous use of: (i) different polarization procedures (i.e., chronoamperometry, chronopotentiometry and cyclic voltammetry) for the monitoring of the charge-transfer reactions taking place at the solid electrolyte/catalyst/gas interface, and (ii) near-ambient pressure photoemission spectroscopy for the in-situ monitoring of the gas-exposed catalyst surface and, in particular, the evolution of potassium coverage. The joint application of these procedures has permitted not only to control the amount of promoter supplied to the catalyst but also to get detailed information about the diffusion processes taking place. This information is deemed of high interest to develop more efficient electro-promoted catalyst systems based on the EPOC phenomena. Knowing the stability and kinetic evolution of the promoter element allows determining its effect on the final performance of the electrocatalyst and the optimal promoting operation conditions.

Acknowledgement

The authors thank the European Regional Development Funds program (EU-FEDER) and the MINECO-AEI (Projects MAT2013-40852-R, 201560E055 and MAT2016-79866-R) for financial support. The NAPP experiments have been carried out in the ALBA synchrotron, Barcelona (Spain).

Appendix A. Supplementary material

Supplementary data associated with this article can be found, in the online version, at https://doi.org/10.1016/j.jcat.2017.11.027.

References

[1] P. Vernoux, L. Lizarraga, M.N. Tsampas, F.M. Sapountzi, A. De Lucas-Consuegra, J.L. Valverde, S. Souentie, C.G. Vayenas, D. Tsiplakides, S. Balomenou, E.A. Baranova, Chem. Rev. 113 (2013) 8192–8260.
[2] A. de Lucas-Consuegra, Catal. Surv. Asia 19 (2015) 25–37.
[3] M. Stoukides, C.G. Vayenas, J. Catal. 70 (1981) 137–146.
[4] J. González-Cobos, A. de Lucas-Consuegra, Catalysts 6 (2016).
[5] R.M. Lambert, M. Tikhov, A. Palermo, I.V. Yentekakis, C.G. Vayenas, Ionics 1 (1995) 366–376.
[6] R.M. Lambert, A. Palermo, F.J. Williams, M.S. Tikhov, Solid State Ionics 136–137 (2000) 677–685.
[7] F.J. Williams, A. Palermo, S. Tracey, M.S. Tikhov, R.M. Lambert, J. Phys. Chem. B 106 (2002) 5668–5672.
[8] F.J. Williams, A. Palermo, M.S. Tikhov, R.M. Lambert, Surf. Sci. 482–485 (2001) 177–182.
[9] F.J. Williams, M.S. Tikhov, A. Palermo, N. Macleod, R.M. Lambert, J. Phys. Chem. B 105 (2002) 2800–2808.
[10] R.M. Lambert, F. Williams, A. Palermo, M.S. Tikhov, Top. Catal. 13 (2000) 91–98.
[11] F.J. Williams, A. Palermo, M.S. Tikhov, R.M. Lambert, J. Phys. Chem. B 103 (1999) 9960–9966.
[12] L. Lukashuk, K. Föttinger, E. Kolar, C. Rameshan, D. Teschner, M. Hävecker, A. Knop-Gericke, N. Yigit, H. Li, E. McDermott, M. Stöger-Pollach, G. Rupprechter, J. Catal. 344 (2016) 1–15.
[13] A. de Lucas-Consuegra, A. Caravaca, P.J. Martínez, J.L. Endrino, F. Dorado, J.L. Valverde, J. Catal. 274 (2010) 251–258.
[14] J. González-Cobos, V.J. Rico, A.R. González-Elipe, J.L. Valverde, A. de Lucas-Consuegra, ACS Catal. 6 (2016) 1942–1951.
[15] J. González-Cobos, J.L. Valverde, A. de Lucas-Consuegra, Int. J. Hydrogen Energy 42 (2017) 13712–13723.
[16] A. Barranco, A. Borras, A.R. Gonzalez-Elipe, A. Palmero, Prog. Mat. Sci. 76 (2016) 59–153.
[17] L. González-García, J. Parra-Barranco, J.R. Sánchez-Valencia, A. Barranco, A. Borrás, A.R. González-Elipe, M.C. García-Gutiérrez, J.J. Hernández, D.R. Rueda, T.A. Ezquerra, Nanotechnology 23 (2012).
[18] R. Alvarez, C. Lopez-Santos, J. Parra-Barranco, V. Rico, A. Barranco, J. Cotrino, A. R. Gonzalez-Elipe, A. Palmero, J. Vac. Sci. Technol. B: Microelectron. Nanometer Struct. 32 (2014).
[19] J.H. Scofield, J. Electron Spectrosc. Relat. Phenom. 8 (1976) 129–137.
[20] S. Tanuma, C.J. Powell, D.R. Penn, Surf. Interface Anal. 43 (2011) 689–713.
[21] R.M. Navarro, M.A. Peña, J.L.G. Fierro, Chem. Rev. 107 (2007) 3952–3991.
[22] C.D. Wagner, G.E. Muilenberg, Handbook of X-ray Photoelectron Spectroscopy: A Reference Book of Standard Data for Use in X-ray Photoelectron Spectroscopy, Physical Electronics Division, Perkin-Elmer Corp, 1979.
[23] X. Guo, Y. Sun, Y. Yu, X. Zhu, C.J. Liu, Catal. Commun. 19 (2012) 61–65.
[24] T. Haga, Y. Nishiyama, J. Catal. 140 (1993) 168–172.
[25] C.G. Vayenas, S. Brosda, Top. Catal. 57 (2014) 1287–1301.
[26] M. Kusche, F. Enzenberger, S. Bajus, H. Niedermeyer, A. Bösmann, A. Kaftan, M. Laurin, J. Libuda, P. Wasserscheid, Angew. Chem., Int. Ed. 52 (2013) 5028–5032.
[27] B. Liu, T. Huang, Z. Zhang, Z. Wang, Y. Zhang, J. Li, Catal. Sci. Technol. 4 (2014) 1286–1292.
[28] A. Caballero, J.P. Espinós, A. Fernández, L. Soriano, A.R. González-Elipe, Surf. Sci. 364 (1996) 253–265.
[29] W. Kuch, M. Schulze, W. Schnurnberger, K. Bolwin, Surf. Sci. 287–288 (1993) 600–604.

[30] E. Ruiz, D. Cillero, Á. Morales, G.S. Vicente, G. De Diego, P.J. Martínez, J.M. Sánchez, Electrochim. Acta 112 (2013) 967–975.
[31] N. Kotsionopoulos, S. Bebelis, J. Appl. Electrochem. 40 (2010) 1883–1891.
[32] G.A. Somorjai, Introduction to Surface Chemistry and Catalysis, John Wiley and Sons Inc, New York, 1994.
[33] C.G. Vayenas, S. Bebelis, M. Despotopoulou, J. Catal. 128 (1991) 415–435.
[34] A. de Lucas-Consuegra, F. Dorado, J.L. Valverde, R. Karoum, P. Vernoux, J. Catal. 251 (2007) 474–484.